



30th Eurosensors Conference, EUROSENSORS 2016

TiO₂ Nanocrystals Decorated CVD Graphene based Hybrid for UV-light Active Photoanodes

C. Ingrosso^{a,*}, G. V. Bianco^{b,†}, V. Pifferi^c, P. Guffanti^c, F. Petronella^a, R. Comparelli^a,
A. Agostiano^{a,d}, M. Striccoli^a, I. Palchetti^e, L. Falciola^c, M. L. Curri^a and G. Bruno^b

^aCNR-IPCF Sez. Bari, c/o Dipartimento di Chimica, Università di Bari, via Orabona 41-70126 Bari, Italy

^bCNR-NANOTEC, c/o Dipartimento di Chimica, Università di Bari, via Orabona 41-70126 Bari, Italy

^cUniversità degli Studi di Milano, Dipartimento di Chimica, via Golgi 19, 20133, Milano

^dDipartimento di Chimica, Università di Bari, via Orabona 41-70126 Bari, Italy.

^eDipartimento di Chimica Ugo Schiff, Università degli Studi di Firenze, via della Lastruccia 3-13, 50019 Sesto Fiorentino (Fi), Italy

Email: c.ingrosso@ba.ipcf.cnr.it

[†] these authors have equally contributed

Abstract

In this work, the manufacturing and characterization of an optically transparent and UV-light photoactive anode, formed of graphene grown by chemical vapor deposition (CVD) decorated with a close packed multilayer nanostructured layout of colloidal TiO₂ nanocrystals (NCs), has been reported. The hybrid material was prepared by a facile solution-based procedure, which relies on incubating the CVD graphene in a solution of 1-pyrene butyric acid (PBA)-surface coated TiO₂ NCs. Pyrene undergoes π - π stacking interactions, anchoring the NCs to the graphene platform with retention of the NC geometry and composition. Concomitantly, the NCs immobilize onto graphene preserving the structure of the aromatic platform. Photoelectrochemical investigation shows that the composite material exhibits a photoelectric response 50% higher than that of bare graphene based electrodes.

© 2016 Published by Elsevier Ltd. This is an open access article under the CC BY-NC-ND license (<http://creativecommons.org/licenses/by-nc-nd/4.0/>).

Peer-review under responsibility of the organizing committee of the 30th Eurosensors Conference

Keywords: colloidal nanocrystals, CVD graphene, hybrid material, UV active photoanode

1. Introduction

Since its first isolation, graphene has attracted scientific community for its unique structural properties, as optical transparency from visible to infrared, excellent thermal and electrical conductivity, high specific surface area, good biocompatibility, impermeability to gases and high strength, elasticity, stiffness and environmental stability [1]. Such functionalities are fully exploited in devices and systems, as field-effect transistors (FETs), sensors, supercapacitors,

touch panels, lithium-ion batteries, conductive inks, field emitters and solar cells [2]. In addition, the high reactivity of graphene offers the opportunity of implementing a large variety of chemical routes of functionalization with other nanostructured compounds. In the resulting nanocomposite materials, the synergic combination of properties of the single components provides materials exhibiting novel functionalities that graphene does not intrinsically possess (i.e. light harvesting in the visible and infrared spectral range, selective molecular recognition capability) or improve its original properties, with enhanced electrical, mechanical and thermal properties and higher capabilities for light-matter interaction based mechanisms [3].

Colloidal nanocrystals (NCs) or nanoparticles (NPs), prepared by means of solution-based colloidal chemistry routes, are optimal candidates for graphene functionalization. Such nanostructured materials are tiny portion of inorganic matter, which exhibits unique size- and shape-dependent optoelectronic properties at the nanoscale [4], which can be conveyed to graphene, resulting in hybrid materials with outstanding functionalities, promising for advanced technological applications. In particular, NCs/NPs prepared by colloidal routes are surface coated by surfactant molecules that can be tuned according to the surface functionalization procedure in order to modulate their chemical interactions with surrounding structures.

Here, a facile method has been used to chemically functionalize graphene, grown by chemical vapor deposition (CVD), with 1-pyrene butyric acid (PBA)-coated TiO₂ NCs. CVD is the most suited method for preparing graphene for mass production and industrial purposes. Indeed, CVD graphene is a scalable material, which can be transferred onto several substrates (i.e. glass, silicon or polymer substrates) also in multilayers [5]. On the other hand, TiO₂ is a wide band gap semiconductor, widely used in (photo)electrochemical sensors, solar cells and photocatalytic systems for its low toxicity, optical transparency, low cost, biocompatibility, photostability and for its photocatalytic and photoelectrochemical activity [6]. Therefore, the synergic combination between the ballistic charge transport and electron sink properties of graphene with the UV-light light harvesting ability of the TiO₂ NCs has been found to provide hybrid materials with enhanced electrical conductivity, photoelectrical conversion efficiency, photocatalytic properties and environmental stability [7].

Here, pre-synthesized oleic acid (OLEA)-coated TiO₂ NCs have been surface functionalized with 1-pyrene butyric acid (PBA), upon a capping exchange procedure aiming to displace the insulating pristine OLEA ligand. The PBA molecule, coordinating the surface of the nano-objects by carboxyl group, is expected to provide the immobilization of the NCs onto the surface of graphene by π - π stacking interactions [8]. The prepared PBA-coated TiO₂ NC modified graphene has been characterized by means of TEM, AFM, Raman spectroscopy and (photo)electrochemical analysis in order to investigate morphology, structure and (photo)electrochemical properties of the nanocomposite. The results indicate that PBA is effective in anchoring the NCs onto graphene, without any significant modification of its structure, ensuring electrically interconnection among the nano-objects by π - π interactions. In addition, PBA plays a crucial role in the electronical coupling, acting as a channel for the charge transfer between the two hybrid components [8]. Indeed, the hybrid material exhibits photoelectrochemical light-energy conversion improved with respect to that of neat graphene, thus resulting suited as UV-light photoactive component of optically transparent electrodes for solar cells, photodetectors, FETs and sensors.

2. Experimental Section

Oleic acid (OLEA)-capped spherical TiO₂ NCs, were synthesized with a diameter of 6 nm under N₂ atmosphere by using a standard air free technique [9]. After the synthesis, the TiO₂ NCs were repeatedly washed with methanol by centrifugation cycles and exposed to a solution of 1-pyrene-butyric acid (BPA) in 1:5 TiO₂/PBA molar ratio, to displace the OLEA ligand with PBA and then finally dispersed in chloroform.

Monolayer graphene with 50-110 μm^2 grain sizes was grown by CVD on 25 μm thick copper foils (Alfa Aesar, item No. 13382) in a typical quartz tube CVD reactor at 1000°C using CH₄/H₂ as precursors. The prepared graphene was then transferred onto 300 nm SiO₂/Si or ITO/glass substrates by using a thermal release tape and a water solution of ammonium persulfate (0.1 M) as copper etchant. Before graphene transfer, the SiO₂/Si substrates were treated with O₂ plasma for improving adhesion. Bilayer graphene was fabricated by transferring of additional graphene layers onto ITO/glass substrates. All graphene samples were dipped in toluene/ethanol/anisole (1/1/1) solution for removing any

organic impurities of thermal tape traces.

Large area graphene transferred on SiO₂/Si substrate was incubated in a 10⁻³ M chloroform solution of PBA-capped TiO₂ NCs for 48 h and finally rinsed with chloroform to remove the NCs not specifically adsorbed.

Topography and phase mode AFM measurements were performed in air and at room temperature, by means of a PSIA XE-100 SPM system operating in tapping mode. A silicon SPM sensor for noncontact AFM (Park Systems), having a spring constant of 42 N m⁻¹ and a resonance frequency of 330 kHz, was used. Topography AFM images were processed by using XEI software to obtain statistical data.

Field emission scanning electron microscopy (FE-SEM) was performed by a Zeiss Sigma microscope operating in the range 0-10 keV and equipped with an in-lens secondary electron detector and an INCA Energy Dispersive Spectroscopy (EDS) detector. Samples were mounted onto stainless-steel sample holders by double-sided carbon tape and grounded by silver paste

Raman spectra of graphene were collected by using a LabRAM HR Horiba-Jobin Yvon spectrometer with a 532 nm excitation laser source. Measurements were carried out under ambient conditions at a low laser power (1 mW) to prevent laser-induced damage. The Raman band recorded from a silicon wafer at 520 cm⁻¹ was used to calibrate the spectrometer, and accuracy of the spectral measurement was estimated to be 1 cm⁻¹.

Photocurrent measurements, performed according to the method already optimized in literature [10] were made at 1 V, illuminating the working electrode at definite times with an UV Jelosil HG500 iron halogenide lamp. All the measurements were carried out in N₂ atmosphere after degassing the cell with nitrogen flow for at least 10 min. Results were normalized subtracting the lower photocurrent curve in order to compare the different photoelectrochemical responses.

3. Results and Discussion

Oleic acid (OLEA)-coated TiO₂ NCs have been synthesized by the colloidal chemistry route reported in [9] and then their surface chemistry was suitably modified, by exchanging the pristine organic capping with 1-pyrene-butyric acid (PBA). Panel A of **Figure 1** shows the TEM image of the achieved PBA-coated TiO₂ NCs. The NCs appear spherical in shape and with an average diameter of 6 nm, thus showing the retention of the typical morphology of the pristine OLEA-coated TiO₂ NCs [9] after surface treatment with PBA. The same panel displays also their UV-vis spectrum characterized by the typical unstructured UV-vis absorption line-shape of the high band gap TiO₂ [9] and points out the optical transparency of the solution, which confirms the lack of aggregation phenomena among the PBA-treated NCs.

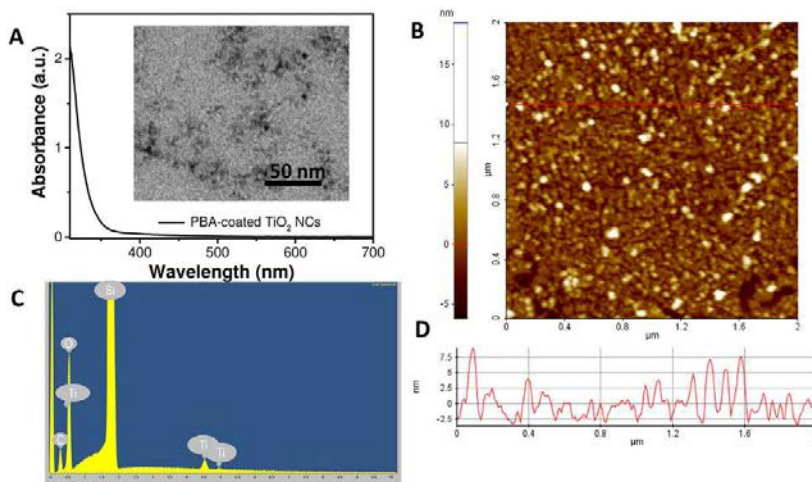


Fig. 1. (A) UV-vis absorption spectrum and (in the inset) TEM micrograph of PBA-coated TiO₂ NCs. (B) 2D topography AFM image and (C) EDS spectrum in the range of 0-6 keV of CVD monolayer graphene functionalized with PBA-capped TiO₂ NCs. (D) Cross sectional line profile taken along the red line of panel B.

A stable dispersion of the PBA-coated TiO₂ NCs has been used to functionalize both monolayer and bilayer CVD graphene films supported on SiO₂/Si. Graphene based films have been incubated in the dispersion of the PBA-coated TiO₂ NCs and then rinsed with pure chloroform to remove the NCs aspecifically adsorbed.

The morphology of the CVD graphene has been investigated before and after functionalization with the PBA-capped TiO₂ NCs [8]. CVD graphene film exhibits a relatively flat and smooth surface morphology [8], but after treatment with the PBA-coated TiO₂ NCs its topography significantly changes. Namely, the AFM image reported in panel B of Figure 1 evidences that the morphology of the hybrid is mainly characterized by a dense and closely interconnected nanoporous layer of grain-type features, having heights up to tens nm. The comparison between the NC size, estimated by the TEM image reported in panel A, and the dimension of the features imaged in panel B leads to infer the arrangement of the PBA-coated TiO₂ NCs in a random close packed nanoporous multilayer structure.

Secondary electron microscopy micrograph provides an overview of the large area arrangement of the NCs in a highly interconnected layer (data not shown). The PBA-coated TiO₂ NCs modified graphene sample has been investigated by EDS analysis recorded in the range between 0-10 keV (Figure 1 C). The spectrum shows the typical K α line of O (0.525 keV) and Ti (4.512 keV) elements, thus further attesting for the deposition of the TiO₂ NCs on graphene.

The films of CVD graphene have been analysed also by Raman spectroscopy and van der Pauw Hall electrical measurements, before and after decoration with the PBA-capped TiO₂ NCs. **Figure 2** reports the Raman spectra of the monolayer CVD-graphene transferred on SiO₂/Si substrate as bare (black line) and functionalized with the PBA-capped TiO₂ NCs (red line). The Raman spectrum shows the typical G and 2D peaks of graphene, which are located at 1583 cm⁻¹ and 2678 cm⁻¹, respectively. After decoration by the PBA-coated TiO₂ NCs, the G and 2D peak positions, as well as the ratio between their intensities drastically change. Namely, the G and 2D Raman peaks shift toward higher wavenumbers, namely from 1583 cm⁻¹ to 1592 cm⁻¹ and from 2678 cm⁻¹ to 2684 cm⁻¹, demonstrating a change of the graphene electronic properties attributed to the increase of the hole carrier concentration in the organic platform, as demonstrated by Das and coworkers [11]. Finally, the three new peaks indicated by the stars in Figure 2 are accounted for the typical Raman peaks of pyrene [12].

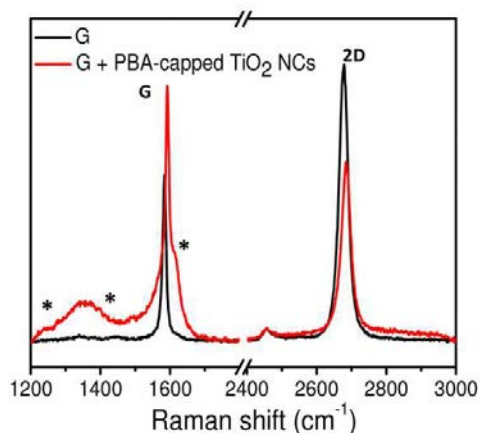


Fig. 2. Raman spectra of CVD monolayer graphene transferred on SiO₂/Si as bare and functionalized with PBA-capped TiO₂ NCs.

Hall measurements show a slight hole-doping effect of the pristine CVD monolayer graphene, ascribed to adsorption of air contaminants, such as H₂O and CO₂ acting as electron-withdrawing species [13]. In particular, the estimated hole concentration of the pristine graphene, n is ca. $1.06 \cdot 10^{12}$ cm⁻², that results in a shift of the graphene Fermi level (ΔE_F , referring to the Dirac point) of 0.12 eV, as derived by the following equation [14]:

$$\Delta E_F = h * v_F \left(\frac{n}{4\pi} \right)^{1/2}$$

where v_F is the Fermi velocity of 1.1×10^8 cm s⁻¹.

After immobilization of the PBA-TiO₂ NCs, the hole concentration is found to further increase up to $2.13 \times 10^{12} \text{ cm}^{-2}$, providing a ΔE_F of 0.17 eV and a decrease of the graphene sheet resistance from 1670 Ohm sq^{-1} to 834 Ohm sq^{-1} , without no substantial effects on the material charge carrier mobility (around $3500 \text{ cm}^2 \text{ V}^{-1} \text{ s}^{-1}$). This finding can be accounted for by a hole transfer from the nano-oxide to graphene, which is induced by the work function mismatch between graphene ($\approx 4.5 \text{ eV}$) and the TiO₂ semiconductor ($\approx 5.58 \text{ eV}$), as previously demonstrated by Liu et al. [15]. It is expected that the short chain aromatic pyrene linker acts as a channel of the hole that are transferred from the TiO₂ NCs to graphene [8].

Transmittance spectra of the CVD graphene modified with the PBA-coated TiO₂ NCs have demonstrated the UV-vis featureless absorption of the hybrid material in the visible spectral range (data not reported) attesting for the optical transparency of the material.

The light-energy conversion properties of the PBA-coated TiO₂ NC modified graphene have been investigated by photoelectrochemical measurements under UV-light illumination in a three-electrode electrochemical cell by using a 0.1 M solution of NaClO₄ as a supporting electrolyte. Working electrodes have been prepared by transferring CVD monolayer and bilayer graphene on Indium Tin Oxide (ITO) glass supporting substrates and modifying them upon soaking in the PBA-TiO₂ NCs solution, as described in the Experimental Section. Namely, PBA-capped TiO₂ NC functionalized monolayer and bilayer graphene films are here indicated as G monolayer + TiO₂ NCs and G bilayer + TiO₂ NCs, respectively. As references of the working electrodes, ITO electrodes modified with pristine monolayer (G monolayer) and pristine bilayer graphene (G bilayer), respectively were prepared.

Figure 3 reports the photocurrent density of the manufactured working electrodes formed of bare and of PBA-coated TiO₂ NCs functionalized graphene, under illumination with an UV-lamp ($\lambda = 356 \text{ nm}$) at the bias voltage of 1V. As it can be noticed, all the *I-t* curves are anodic, attesting for the occurrence of oxidation of the medium, with concomitant transfer of photogenerated electrons from the photoanode hybrid material to ITO. Bare graphene based working electrodes have a photocurrent density originated from the $\pi-\pi^*$ transition of the graphene C=C bond [16] occurring under UV-light. In particular, the bilayer graphene shows a photocurrent density higher than that of the monolayer, namely $0.30 \mu\text{A cm}^{-2}$ against $0.15 \mu\text{A cm}^{-2}$, explained by the linear increase of the broadband absorption of graphene for increasing number of layers.

Upon immobilization of the PBA-coated TiO₂ NCs on graphene, the working electrodes show an improvement of the photocurrent density. Such a finding is particularly evident in the case of the modified bilayer graphene, with a photocurrent density increased up to $0.45 \mu\text{A cm}^{-2}$. This result is ascribed to the intrinsic UV-light photo-activity of the TiO₂ NCs film which provides generation and separation of electron-hole pairs, that are then transferred to graphene through pyrene. Indeed, pyrene linker stabilizes the photoelectrons by its π ring system and transfers them to graphene, where they are stored in the huge $\pi-\pi$ network of the aromatic platform. In addition, the Fermi level of graphene lies in between the conduction band of TiO₂ and that of ITO, and hence it decreases the injection barrier at the ITO/TiO₂ NCs interface. Finally, graphene, behaving as a charge acceptor and fast carrier transporter, facilitates separation of the photoexcited electron-hole pairs and enables photoelectron withdrawal from the NC oxide film to ITO supporting electrode, suppressing both recombination processes at the defect states of the NC oxide film and back reactions at the interface with the electrolyte [17]. Such a merging of functionalities between the hybrid components results in an overall improved photoelectric conversion efficiency.

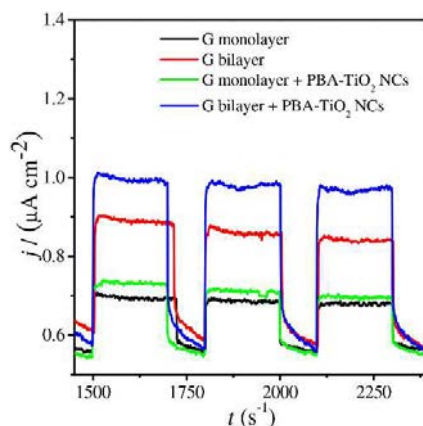


Fig. 3. (A) Photocurrent density transient measurements collected under UV-light ($\lambda=365$ nm) irradiation of ITO electrodes modified with monolayer graphene (G monolayer), bilayer graphene (G bilayer) and PBA-TiO₂ NC functionalized monolayer and bilayer graphene (G monolayer + TiO₂ NCs and G bilayer + TiO₂ NCs).

4. Conclusion

An optically transparent and UV-light photoactive anode, based on a hybrid material formed of a large area CVD grown graphene film chemically functionalized with colloidal TiO₂ NCs, has been manufactured by a facile solution-based approach.

The photoactive hybrid material has been fabricated by chemical immobilization of the TiO₂ NCs, surface functionalized with the aromatic ligand 1-pyrene butyric acid (PBA) after a capping exchange procedure performed on pre-synthesized NCs, on the CVD graphene.

TiO₂ NCs assemble in a multilayer nanoporous layout, thanks to π - π stacking forces, onto the graphene platform retaining its structural properties. Concomitantly, ligand π - π interactions among the pyrene molecules capping the NCs provide a highly interconnection along the nanostructured porous film.

The TiO₂ NC film acts as a p-doping layer increasing graphene electrical conductivity and light-to-charge conversion capability.

The manufactured optically transparent photoanode are potentially relevant for integration in photoelectrochemical sensors, solar cells and photodectors. The photoactivity of the hybrid material can be exploited in photoelectrochemical sensors for providing red/ox processes and detecting (bio)molecules. The highly nanoporous multilayer layout of PBA-coated TiO₂ NCs provide a high surface area for QD immobilization, thus extending light harvesting ability of the composite in the visible and infrared spectral region for highly performing solar cells and photodectors. Moreover, the photoactivity of the hybrid can result interesting for promoting catalytic processes.

Finally, the same approach can be extended to the immobilization of other types of nanoparticles with diverse composition (metal, oxide and chalcogenides) and coordinated by pyrene ligands having different end functional groups, for manufacturing composites exhibiting interesting functionalities, with a relevant potential for a wide range of advanced technological applications.

Acknowledgements

The authors acknowledge the Italian PRIN 2012 (prot.20128ZZS2H), Italian Regional Network of Laboratories "Sens&Micro" (POFESR 2007-2013) and Italian PRIN 2012 (prot.2012T9XHH7) projects.

References

1. S. Stankovich, D. A. Dikin, G. H. B. Dommett, K. M. K. Kohlhaas, E. J. Zimney, E. A. Stach, R. D. Piner, S. T. Nguyen, R. S. Ruoff, Graphene-Based Composite Materials, *Nature* 442 (2006) 282-286.
2. J. T. Han, B. J. Kim, B. G. Kim, J. S. Kim, B. H. Jeong, H. J. Jeong, S. Y. Jeong, J. H. Cho, G.-W. Lee, Enhanced Electrical Properties of Reduced Graphene Oxide Multilayer Films by In-Situ Insertion of a TiO₂ Layer, *ACS Nano* 5 (2011) 8884-8891.
3. V. Georgakilas, J. N. Tiwari, K. C. Kemp, J. A. Perman, A. B. Bourlinos, K. S. Kim, R. Zboril, Noncovalent Functionalization of Graphene and Graphene Oxide for Energy Materials, Biosensing, Catalytic, and Biomedical Applications, *Chem. Rev.* 116 (2016) 5464-5519.
4. A. P. Alivisatos, Semiconductor Clusters, Nanocrystals, and Quantum Dots, *Science* 271 (1996) 933-937.
5. Q. Yu, L. A. Jauregui, W. Wu, R. Colby, J. Tian, Z. Su, H. Cao, Z. Liu, D. Pandey, D. Wei, T. F. Chung, P. Peng, N. P. Guisinger, E. A. Stach, J. Bao, S. S. Pei, Y. P. Chen, Control and characterization of individual grains and grain boundaries in graphene grown by chemical vapour deposition, *Nat. Mater.* 10 (2011) 443-449.
6. V. Pifferi, G. Soliveri, G. Panzarasa, S. Ardizzone, G. Cappelletti, D. Meroni, L. Falciola, Electrochemical sensors cleaned by light: a proof of concept for on site applications towards integrated monitoring systems, *RSC Advances* 5 (2015) 71210-71214.
7. H. J. Jeong, H. Y. Kim, H. Jeong, J. T. Han, S. Y. Jeong, K.-J. Baeg, M. S. Jeong, G.-W. Lee, One-Step Transfer and Integration of Multifunctionality in CVD Graphene by TiO₂/Graphene Oxide Hybrid Layer, *Small* 10 (2014) 2057-2067.
8. C. Ingrosso, G. V. Bianco, M. Corricelli, R. Comparelli, D. Altamura, A. Agostiano, M. Striccoli, M. Losurdo, M. L. Curri, G. Bruno, Photoactive Hybrid Material Based on Pyrene Functionalized PbS Nanocrystals Decorating CVD Monolayer Graphene, *ACS Appl. Mater. & Interfaces* 7 (2015) 4151-4159.
9. P. D. Cozzoli, A. Kornowski, H. Weller, Low-temperature synthesis of soluble and processable organic-capped anatase TiO₂ nanorods, *J. Am. Chem. Soc.* 125 (2003) 14539-14548.
10. F. Spadavecchia, G. Cappelletti, S. Ardizzone, M. Ceotto, M. S. Azzola, L. Lo Presti, G. Cerrato, L. Falciola, Role of Pr on the Semiconductor Properties of Nanotitania. An Experimental and First-Principles Investigation, *J. Phys. Chem. C* 116 (2012) 23083-23093.
11. A. Das, S. Pisana, B. Chakraborty, S. Piscanec, S. K. Saha, U. V. Waghmare, K. S. Novoselov, H. R. Krishnamurthy, A. K. Geim, A. C. Ferrari, A. K. Sood, Monitoring Dopants by Raman Scattering in an Electrochemically Top-gated Graphene Transistor, *Nat. Nanotechnol.* 3 (2008) 210-215.
12. Y. Shinohara, K. Yamakita, K. Ohno, Raman spectra of polycyclic aromatic hydrocarbons. Comparison of calculated Raman intensity distributions with observed spectra for naphthalene, anthracene, pyrene, and perylene, *J. Mol. Struct.* 442 (1998) 221-234.
13. M. Lafkioti, B. Krauss, T. Lohmann, U. Zschieschang, H. Klauk, K. Klitzing, J. H. Smet, Graphene on a Hydrophobic Substrate: Doping Reduction and Hysteresis Suppression under Ambient Conditions *Nano Lett.* 10 (2010) 1149-1153.
14. Y. Si, E. T. Samulski, Synthesis of water soluble graphene, *Nano Lett.* 8 (2008) 1679-1682.
15. X. Liu, R. Cong, L. Cao, S. Liu, H. Cui, The structure, morphology and photocatalytic activity of graphene-TiO₂ multilayer films and charge transfer at the interface, *New J. Chem.* 38 (2014) 2362-2367.
16. L. Li, X. Zheng, J. Wang, Q. Sun, Q. Xu, Solvent-Exfoliated and Functionalized Graphene with Assistance of Supercritical Carbon Dioxide, *ACS Sustainable Chem. Eng.* 1 (2013) 144-151.
17. N. Yang, J. Zhai, D. Wang, Y. Chen, L. Jiang, Two-Dimensional Graphene Bridges Enhanced Photoinduced Charge Transport in Dye-Sensitized Solar Cells, *ACS Nano* 4 (2010) 887-894.